Twenty-Sixth Symposium (International) on Combustion/The Combustion Institute, 1996/pp. 1171–1179

THIN-FILAMENT PYROMETRY IN FLICKERING LAMINAR DIFFUSION FLAMES

WILLIAM M. PITTS
Building and Fire Research Laboratory
National Institute of Standards and Technology
Gaithersburg, MD 20899, USA

This paper describes an experimental system for thin-filament pyrometry (TFP) in acoustically phase-locked flickering laminar methane/air diffusion flames. The physical basis of the technique is discussed. The experiment utilizes a 15-μm β-SiC fiber, which is simultaneously imaged at 540 points over a length of 27.5 mm using a cooled CCD camera. This arrangement provides measurements over a 1200–2100-K temperature range having a spatial resolution of $\sim$100 μm, a temporal resolution of 1.5 ms, and a precision of 1.5 $\pm$ 1.0 K for temperatures on the order of 2000 K. The TFP is calibrated assuming that the strongest filament emission at a height 7 mm above the burner for a steady laminar flame corresponds to a temperature of 2000 K. Temperatures at different positions along the filament are then determined by recording relative emission intensities and assuming that the filament acts as a gray-body emitter. Measured filament temperature profiles are found to be in good agreement with earlier radiation-corrected thermocouple results by Richardson and Santoro for the same steady laminar flame. The calibrated TFP is then used to make filament temperature measurements at various heights and phases of a previously studied flickering flame entering a low-velocity air flow. The use of a two-dimensional CCD allows a baseline to be determined, and measurements can be made in the presence of background luminosity, which is observed in sooting regions. In order to demonstrate the effectiveness of the approach, measurements are discussed for various heights above the burner and phases of the flickering flame. The need for an extremely well-characterized flame for calibrating TFP is discussed. Knowledge of flow velocities and molecular composition in both the calibration and flickering flames is required to improve the accuracy of flame temperature measurements using TFP.

Introduction

The experimental characterization and modeling of simple flame systems (such as stationary laminar diffusion flames of simple gaseous fuels) has progressed dramatically. Before these advances can be applied to the design of practical devices, it is necessary to develop similarly detailed experimental and modeling approaches for turbulent combustion. As a step in this direction, a coordinated experimental and modeling effort is being used to investigate acoustically phase-locked flickering laminar diffusion flames in order to better characterize and model flame/flow interactions [1–5].

One of the obstacles to this characterization has been the lack of experimental diagnostics for temperature measurement having high spatial and temporal resolution. Recently, thin-filament pyrometry (TFP) has been shown to have potential for providing such measurements [6]. The current work describes the development of a new TFP approach designed especially to allow measurements in the flickering flames, but which is useful for a wider range of combustion applications. This technique provides highly precise, semiquantitative measurements having excellent temporal and spatial resolution. Representative results are presented to demonstrate the effectiveness of TFP.

Thin-Filament Pyrometry

The use of TFP in flames was pioneered by Vilimpoc et al. [6], and the theory and development of the technique is discussed in detail in several publications [7–9] from this group. Bédat et al. [10] have performed similar measurements.

The physical basis of TFP is simple and elegant. The intensity of thermal electromagnetic radiation from a length of heated silicon carbide (β-SiC) fiber is used to characterize the temperature of the fiber and can be related to the temperature of gas surrounding the fiber. These fibers have very small diameters (nominally 15 μm) while having sufficient strength and temperature resistance to survive hours when inserted in typical atmospheric hydrocarbon diffusion flames. Here the necessary physics and past experimental approaches are summarized. References 6–10 should be consulted for additional details.

A heated β-SiC fiber is adequately approximated as a gray body [6–10] for which the spectral emissive power, E_g, can be written as follows [11]:

$$E_g(\lambda, T) = \frac{2\pi\varepsilon hc^2}{\lambda^5[e^{hc/\lambda kT} - 1]} \quad (1)$$

where λ is wavelength, T is temperature, ε is the apparent emissivity for the fiber, h is Planck's constant, c is the speed of light, and k is Boltzmann's constant.

The relative light intensity emitted by the heated fiber is recorded using a photodetector having a wavelength-dependent response function, R. The overall signal, S, generated by the detector as a function of temperature is given as

$$S(T) = k_{\exp} \int_{\lambda_1}^{\lambda_2} E_g(\lambda, T)R(\lambda)d\lambda \quad (2)$$

where $k_{\exp}$ is an experimental coefficient assumed to be independent of wavelength. The wavelength range for the integration covers the sensitivity range of the detector.

Thermal radiation is a strong function of temperature and wavelength. Maximum emissive powers for the high temperatures typical of hydrocarbon flames occur at wavelengths in the mid-infrared, and radiated power decreases rapidly at shorter wavelengths. These variations of E_g with temperature and wavelength have important implications for the effective range and potential accuracy of TFP measurements.

TFP results reported in the literature have used similar experimental approaches [6–10]. The image of a β-SiC fiber strung across a flame was focused onto a rotating mirror that scanned the image of the fiber across a single-element photodetector. The temporal output of the detector therefore corresponded to the measured relative intensity along the fiber, and the temporal resolution was determined by the scan rate of the mirror.

The first TFP measurements [6–9] utilized an InGaAs PIN photodiode that responds to wavelengths from 0.9 to 1.8 μm. Output signals were digitized to 8 bits (1 part in 256). Temperatures over a 1000–2380 K range could be measured with a precision of ± 4 K at high temperatures, but, due to the rapid fall-off of the signal at lower temperatures, the precision was degraded to $\sim \pm 40$ K. Bédat et al. [10] utilized a mid-infrared line scanner equipped with a cooled InSb detector and a narrow-band 3.9-μm filter to limit interference from flame radiation. Eight-bit digitization was also used. Due to their measurement of light intensities at longer wavelengths, these workers were able to detect temperatures as low as 550 K and reported a precision of $\sim \pm 20$ K at 600 K.

Previous investigators have discussed additional properties of β-SiC fibers that are crucial for measuring temperature with high temporal and spatial resolution [6–10]. Temperature differences arise between the sensor and surrounding gases that are determined by a balance of convective heat transfer to the filament and radiative losses. Convective heat transfer depends on the local flow velocity and molecular composition and can be estimated using standard heat-transfer expressions for cylinders. Estimates of these corrections by Goss et al. [8] and Bédat et al. [10] for typical flames with velocities of 2 m/s are 200–400 K at 2000 K, and 40 K at 1200 K.

Heat transfer from the gas to the fiber also limits the rate at which a TFP can respond to temperature changes. Solution of the transient heat-transfer equation allows the time resolution to be estimated. The effective response time also depends on flow velocity and molecular composition. For typical flame conditions, Goss et al. [8] and Bédat et al. [10] provide estimates of $\sim$1 ms. Measurements at room temperature using laser heating were shown to agree well with prediction. The spatial resolution of TFP is limited by longitudinal heat conduction along the fiber. A value of $\sim$100 μm is estimated for high temperatures [8,10]. The earlier experimental systems had scan rates of 1000 [8] to 2500 Hz [10] and spatial resolutions of 120 [8] to 190 μm [10].

Two limitations of TFP as described in the literature should be noted. First, the technique must be calibrated. This requires the availability of a flame system having an accurately known temperature and, for highly accurate measurements, known molecular composition and velocity. Second, the use of a single-element photodetector limits experiments to cases where radiative emission from other sources, such as soot or molecular species, are not present.

Experimental System

Figure 1 is a schematic of the experimental system. The coannular burner [1] is formed by a 1.1-cm-diameter fuel tube surrounded by a 10.2-cm-diameter air flow smoothed by glass beads, several screens, and a ceramic honeycomb. The fuel tube is attached to a plenum containing a loudspeaker used to oscillate the fuel velocity and thus lock the flame flicker frequency at 10 Hz. "CP"-grade methane is used as fuel. The entire burner is mounted on a vertical stage to position the flame relative to the β-SiC filament.

A 115-mm length of nominally 15-μm-diameter β-SiC fiber is stretched between two pieces of metal "shim" stock that provide tension to maintain the fiber taut as its length changes with heating. The fiber is positioned horizontally downstream of the fuel tube and passes through the burner centerline. The fiber is imaged onto a cooled (238 K) CCD camera using a 90 mm f/2.5 lens (f/32 aperture) focused

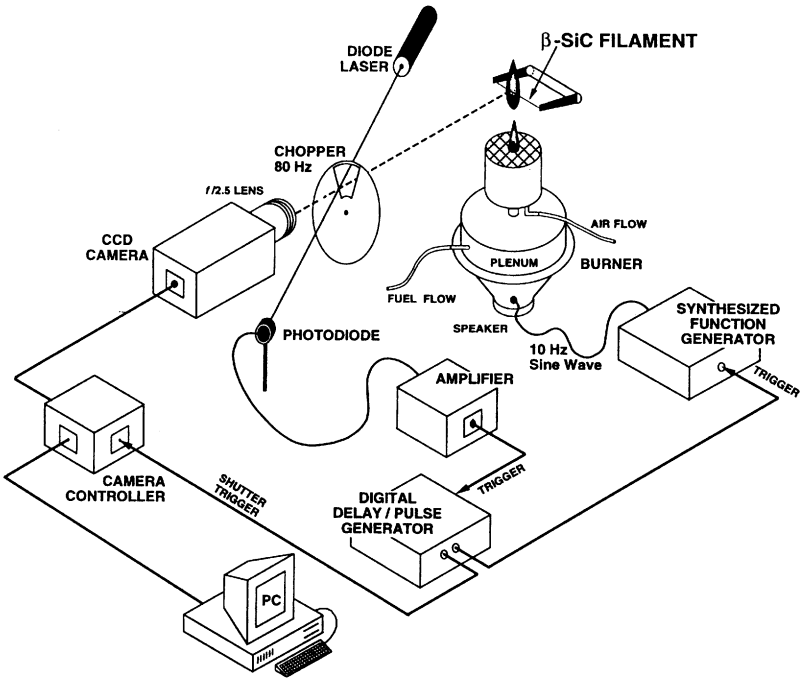

FIG. 1. The experimental system for thin-filament pyrometry in phase-locked flickering laminar diffusion flames is shown.

such that each of the 22 × 22 μm pixels corresponds to 51 × 51 μm in the image plane. A 540 × 61 pixel area of the array having a uniform response was used. Pixel intensities were digitized with 16-bit accuracy and saved in ASCII format for later analysis.

In order to resolve the flickering flame temporally, it is necessary to make TFP measurements with ~1-ms resolution. The electronic shutter provided with the camera cannot be reliably opened for periods less than 10 ms. For this reason, a variable-speed chopper with a blade having a single 5.5-cm-high opening covering 30° was placed in front of the camera lens. When operated at 80 Hz, the chopper provided an effective shutter time of 1.5 ms. The camera's electronic shutter was opened and closed sufficiently fast to ensure that an image was recorded during a single passage of the chopper opening.

A diode laser beam passing through the chopper and an amplified photodiode were used to generate a voltage pulse train at 80 Hz that triggered a digital delay/pulse generator to produce time delays and electronic triggers at 10 Hz for a synthesized function generator, which provided the sine-wave voltage for the loudspeaker, and the camera shutter. The timing was such that initiation of a waveform sweep and the opening of the chopper occurred synchronously.

The flame conditions were those reported by Smyth et al. [1]. The flickering flame was acoustically locked by applying a 10.0-Hz 0.75-V sinusoidal voltage to the loudspeaker to generate moderately flickering conditions. Figure 2 shows two-dimensional images of soot scattering and hydroxyl laser-induced fluorescence recorded previously as a function of phase [3]. The percentages refer to the fraction of a complete cycle relative to an arbitrary initial phase angle. Results for 10 different phase angles are shown. The methane and coflow air nominal velocities of 77.8 and 79.0 mm/s, respectively, were generated by mass-flow controllers accurate to 1%.

The TFP was calibrated as described in the following section using a steady laminar flame. TFP measurements were recorded for several of the phases shown in Fig. 2.

Analysis Procedures

The first step in the determination of temperature from a TFP measurement is recording the emission intensity along the fiber. Figure 3 shows an example of a TFP image. Emission from the filament is clearly visible, but there is also significant flame luminosity due to soot. It is necessary to relate filament emission intensity to temperature in the presence of background light.

Plots of the digitized intensity recorded for pixels perpendicular to the filament direction were least-

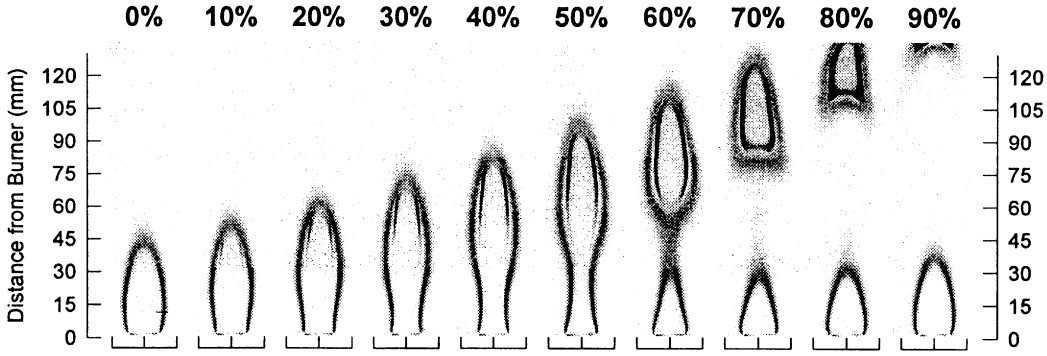

FIG. 2. Two-dimensional sheet images recorded by Shaddix and Smyth [3] of hydroxyl radical laser-induced fluorescence and soot Mie scattering are reproduced for 10 phases of a 10-Hz, phase-locked, flickering laminar diffusion flame of methane entering a coflow of air. Nominal methane and air velocities are 77.8 and 79.0 mm/s, respectively, and a sine wave of 0.75-V amplitude was applied to the loudspeaker. The percentages refer to the fraction of the phase relative to an arbitrarily chosen phase. The soot scattering signals correspond to the darker narrow bands closer to the burner centerline, while the more diffuse signals at the outer edges are due to hydroxyl radical. The scales at the bases of the images cover a lateral distance of 30 mm.

FIG. 3. A 540 × 61 pixel CCD image recorded during a single 1.5-ms passage of the chopper opening shows the thermal emission recorded from a 15-μm β-SiC fiber located within the phase-locked flickering laminar diffusion flame. Flame radiation from soot is also evident. The fiber is positioned 55 mm above the burner exit, and the phase is 30%. Comparison with Fig. 2 shows that there is a significant soot volume fraction in the flame that has been previously measured to have a maximum value of 6.6×10^{-7} for this position and phase [3].

squares fit to both Gaussian and Lorentzian curves. The Lorentzian function provided a much better fit and indicated that the full width half maximum for the fiber image (which is a measure of the spatial resolution for the optical system) was 0.75 pixels or 38 μm. Since the estimated thermal length for the β-SiC fiber is ~100 μm, the latter value determines the effective spatial resolution along the fiber.

The emission intensity at a particular location is obtained by integrating the individual pixel intensities across the filament. In order to correct for a zero offset in the signal and background emission, it is necessary to determine a baseline to be subtracted from the measurements. The sharpness of the image allows the integration to be performed over nine pixels centered on the pixel having the maximum intensity, $[S(T)_{max}]_{i=0}$. A baseline was determined by a linear least-squares-curve fit over readings for three pixels on either side of the integrated region, i.e., for relative pixel numbers −7, −6, −5, 5, 6, and 7. The assumption of a linear baseline has been found to be adequate over the 0.77-mm length used for the calculation.

The above analysis provides relative emission intensities for the 540 pixel locations (total length of 27.5 mm) of the image. The next requirement is to convert relative intensities to temperatures. The first step in this process is to calculate the expected relative signal as a function of filament temperature using Eqs. (1) and (2) along with $R(\lambda)$ for the silicon-based CCD detector (taken from the camera manufacturers' literature).

The integration was performed numerically using Simpson's rule and assuming $\varepsilon = 0.88$ [8]. The results are plotted on a semilog scale in Fig. 4. The CCD has its greatest sensitivity in the near-infrared and visible regions of the spectrum. These wavelengths lie well to the blue of those for the maximum thermal emission at typical flame temperatures as well as the sensitivity ranges of detectors used previously for TFP [6–10]. As a result, predicted values of $S(T)$ vary over more than 10 orders of magnitude for temperatures from 500 to 2000 K. Clearly, it will not be possible to make measurements in the lower temperature range with the current experimental arrangement. The insert in Fig. 4 shows a linear plot of higher temperatures as a function of relative $S(T)$. The solid line is a fifth-order polynomial fit to the

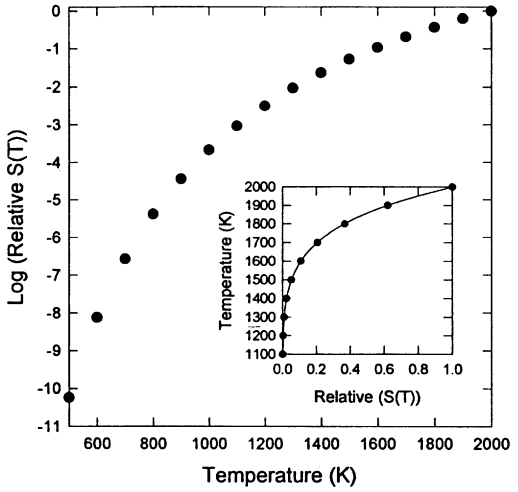

FIG. 4. A semilog plot of relative TFP signal levels, $S(T)$, calculated using Eq. (2), is shown for the case of a silicon CCD array detecting the emission from a heated gray body over a temperature range of 500–2000 K. The insert shows the high-temperature results plotted as temperature versus relative signal. The solid line is the result of a fifth-order polynomial fit to the data, which is used to deduce measured filament temperatures from experimental measurements of $S(T)$.

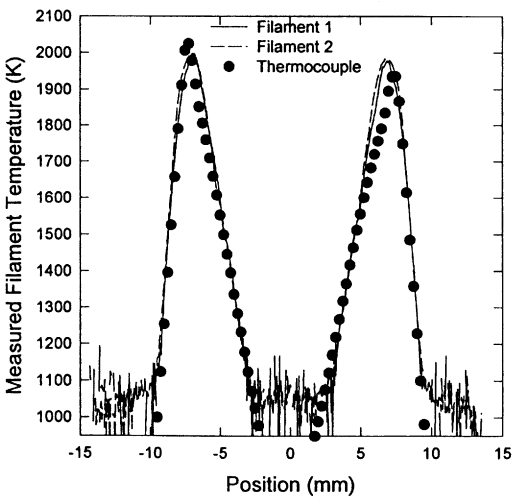

FIG. 5. Measured filament temperatures for two different β-SiC fibers and flame temperatures from radiation-corrected thermocouple measurements [12] are plotted along a line located 7 mm from the burner exit of a steady laminar flame formed by a methane flow into an air coflow. The thin-filament pyrometers have been calibrated by assigning a value of 2000 K to the highest observed emission intensity.

full curve. It reproduces the calculated results quite well and can be used to convert relative values of $S(T)$ to temperature. The conversion should be more precise at high temperatures; however, signal levels should be sufficient to allow meaningful measurements for temperatures as low as 1100–1200 K (see Fig. 4).

Previous investigators have used either estimated temperatures in premixed flames [8] or a modification of the disappearing tungsten filament measurement method [10] to calibrate the device. Neither of these approaches provide accuracies approaching the precision possible for TFP. Due to the lack of a suitable temperature standard and detailed knowledge concerning the flame system under study, an approximate approach has been adopted here. Richardson and Santoro [12] have provided radiation-corrected thermocouple measurements across the steady flame for an identical burner and flow conditions. TFP signals were recorded at a position (7 mm downstream of the burner exit) for which thermocouple measurements are available. Based on their findings, the maximum observed TFP signal has been assigned a value of 2000 K. Once this value is assigned, relative emission intensities and the curve shown in Fig. 4 are used to determine temperatures for other filament locations. The same calibration factor was then applied to temperature measurements in the time-varying flames.

No attempt has been made to correct for the effects of radiation losses. For this reason, the experimental results are reported as measured filament temperatures (MFTs). As shown below, there is a good correlation between MFTs and flame temperatures measured by thermocouples [12].

Results

Only two fibers were required during this investigation. The first broke after several months and many hours within the flame environment. Signal levels were high. Even though the CCD camera lens was used with its smallest aperture, it was necessary to add a 70% transmitting neutral density filter to avoid saturating the detector array.

Figure 5 compares MFTs for the two filaments and the corresponding thermocouple temperature measurements for the steady calibration flame. The MFT curves for high temperatures are smooth, indicating that the precision is high. For MFTs less than 1200 K, the data first become more noisy and then meaningless as the signal levels decrease with decreasing temperature. In later data plots, only MFTs greater than 1200 K will be shown. The high-temperature TFP results agree well with each other and with the thermocouple measurements, suggesting that MFTs are a good approximation for the flame temperature. The thermocouple results are

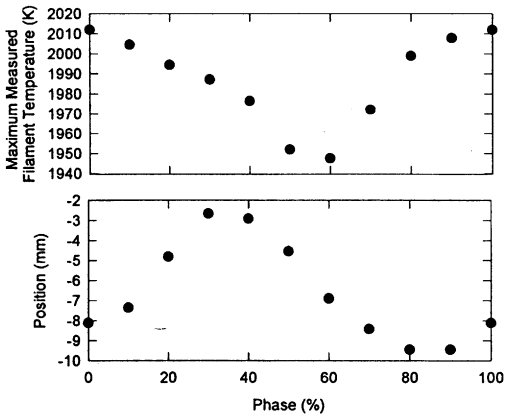

FIG. 6. Values of the maximum observed measured filament temperature and its location for one side of the flickering flame are plotted as a function of the phase of the sine-wave voltage applied to the loudspeaker. The filament is located 7 mm from the burner exit.

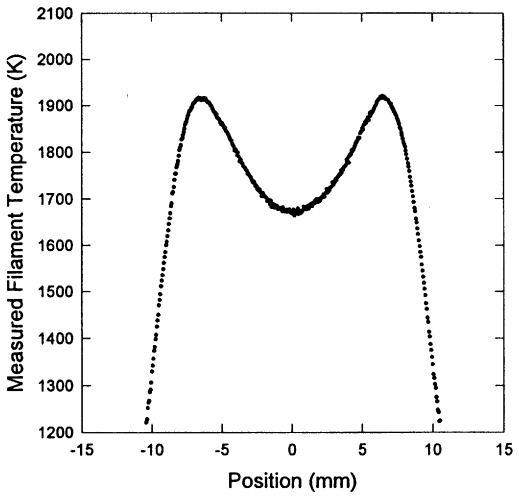

FIG. 7. The measured filament temperature profile determined from the image shown in Fig. 3 is plotted as a function of position across the flickering flame for a location 55 mm from the burner exit and a phase of 30%. The results demonstrate that TFP measurements can be made in the presence of significant soot luminosity.

asymmetric. The maximum temperature of 2000 K chosen for the TFP calibration falls between the two peak temperatures. The agreement of the MFTs with the thermocouple results is excellent on the lean side of the flame, but the TFP results are somewhat higher at high temperatures on the inner, rich sides of the flame. This difference is unexplained.

Close inspection shows that the maximum MFTs on either side of the flame for the first filament differ by roughly 25 K. This difference can be attributed to small variations in the diameter of the fiber. The second fiber seems somewhat more uniform with measured temperature differences on the order of 5 K. Differences in maximum MFTs for a given location observed during 11 repeated measurements on each side of the steady flame, for which only one of the four measurements served for calibration, was 1.4 ± 1.0 (1σ) K. The precision decreases with decreasing temperature and also in cases where there is strong background emission due to soot.

Attempts to measure temperature in the sooting region of the steady flame were thwarted by thermophoretic deposition of soot onto the fiber, which resulted in increased emission and incorrect temperature measurements. Deposited soot could be burned off by placing the fiber in a lean high-temperature region of the flame. No indications of soot deposition were observed in the time-varying flame, presumably due to the fact that soot is repeatedly deposited and oxidized and thus does not have time to accumulate.

Calibrated filaments were used to record MFTs for different phases and vertical positions in the time-varying flame. Measurements 7 mm from the burner exit had similar appearances to the steady flame, but the maximum MFT and its distance from the centerline varied with phase. Figure 6 shows plots of $(\mathrm{MFT})_{max}$ and its position for one side of the flame as a function of the phase. Note that data for each phase are taken from single measurements and that no averaging has been employed. Forcing the flame generates a nearly sinusoidal variation in flame position, while generally decreasing the temperature from that of the unperturbed flame (defined to be 2000 K). The smooth variation of temperature with phase evident in the figure indicates that the precision of the measurements in the time-varying flame approaches that quoted earlier (1.4 ± 1.0 K) for the steady flame. Variations in the high-temperature location with phase are consistent with the flame shapes shown in Fig. 2.

The above measurements were in a region where soot luminosity is unimportant. Figure 7 shows the temperature profile calculated for the filament image reproduced in Fig. 3, where there is a significant luminosity due to soot. The overall shape of the temperature profile is as expected for this location in the flame. The presence of soot and the resulting thermal emission do not interfere with MFT measurements.

Figure 8 compares temperature profiles recorded at 12 heights with the corresponding two-dimensional image for the 60% phase of the forced flame. Some interesting features are the increasing temperature with height for positions near the burner, the high temperatures observed in the "neck" region, the cooling (presumably by radiation) in the clipped-off portion of the flame, and the existence

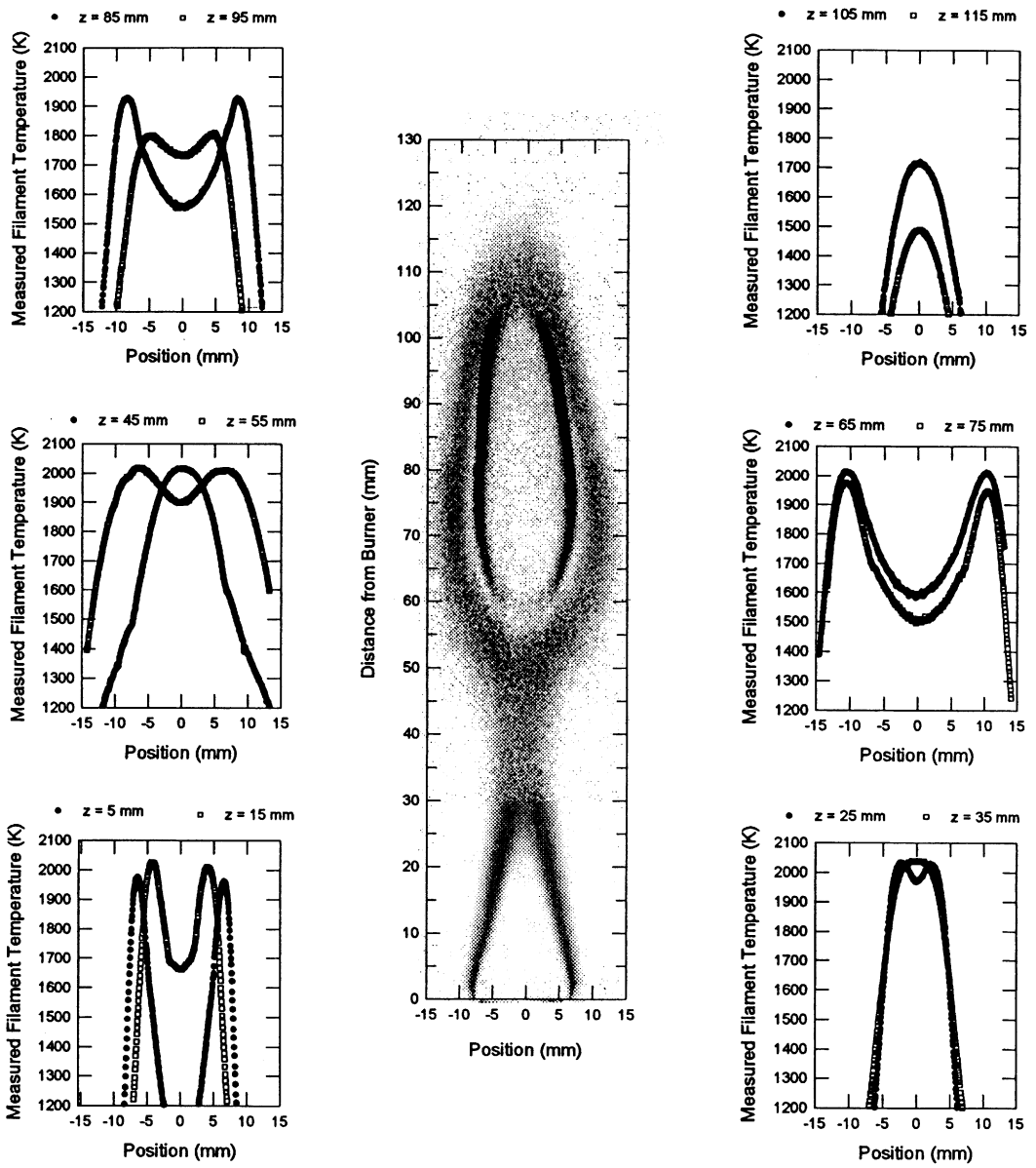

FIG. 8. Radial profiles of measured filament temperature at 12 distances from the burner exit in a flickering methane flame are compared with the corresponding two-dimensional hydroxyl radical fluorescence and soot scattering image (see Fig. 2) for a phase of 60%. The relative radial positions of the profiles have been shifted slightly to remove the effects of minor flame movements.

of heated gases above the obvious luminous zone of the two-dimensional image.

Discussion

It has been shown that TFP is a powerful tool for characterizing time-varying laminar diffusion flames. TFP provides temperature line measurements over a range of 1200–2100 K with a spatial resolution of 100 μm, a temporal resolution of ~1.5 ms, and a precision on the order of 1.5 K at high flame temperatures. The method has been applied in sooting regions of the flickering flame having peak soot volume fractions of 1.8×10^{-6} [2]. The author is

unaware of any other technique that can match this performance.

The TFP system described here differs significantly from previous systems [6–10]. A cooled two-dimensional CCD array is used instead of a single-element detector and a scanning mirror. The major advantage of using the array is that it provides a baseline for correcting for background luminosity. One limitation is that temperature fluctuations cannot be followed in real time. This is not a serious drawback in phase-locked flames, which are highly repetitive. A second limitation of the current system is that the array detects light at shorter wavelengths than the detectors used in earlier investigations. As a result, the observed filament emission varies very strongly with temperature. This limitation is somewhat overcome by measuring light intensities with 16-bit as opposed to the 8-bit resolution used for earlier studies. Even so, it is clear that the dynamic range as well as the precision of the measurements at lower temperatures could be improved significantly by replacing the current detector with one capable of detecting longer wavelength light with similar precision.

Results have been reported as MFTs since they are uncorrected for radiative heat losses. While the comparison of the results with flame temperatures measured by thermocouples (Fig. 5) shows good agreement, it is clear that the accuracy of the measurements is considerably less than their precision. To improve the accuracy, it will be necessary to develop a high-temperature flame calibration system for which temperatures are known accurately to a few degrees or better and which has very well-characterized velocities and composition to allow radiation corrections. The availability of velocities and composition profiles in the time-varying flames either from experiment or modeling will also be required.

The results presented demonstrate the detailed temperature field measurements that are possible. These measurements will allow the characterization of the effects of heat loss, strain fields, and scalar dissipation on the thermal structure of time-varying laminar flames to a degree not possible heretofore. When combined with the findings of companion investigations in the same system [1–5], the results promise to provide an improved understanding of chemical/flow field interactions in diffusion flames, an important step in developing models for turbulent combusting flows.

Acknowledgments

This work was supported by the Basic Research Group of the Gas Research Institute using equipment provided by NIST. The author thanks Larry Goss of Innovative Scientific Solutions, Inc. for providing the β-SiC fibers, Kermit Smyth and David Everest of NIST for helpful discussions and for supplying their previous experimental results, Walter Bowers of NIST for loaning the chopper, Ted Schurter of EG&G for providing the chopper wheel, and Nelson Bryner and Marco Fernandez of NIST for aid in assembling the experiment.

REFERENCES

1. Smyth, K. C., Harrington, J. E., Johnsson, E. L., and Pitts, W. M., *Combust. Flame* 95:229–339 (1993).
2. Shaddix, C. R., Harrington, J. E., and Smyth, K. C., *Combust. Flame* 99:723–732 (1994).
3. Shaddix, C. R. and Smyth, K. C., *Combust. Flame*, in press.
4. Kaplan, C. R., Shaddix, C. R., and Smyth, K. C., *Combust. Flame*, 106:392–405 (1996).
5. Skaggs, R. R. and Miller, J. H., *Fall Technical Meeting of the Eastern States Section of the Combustion Institute*, Clearwater, FL, December 5–7, 1994, pp. 172–175.
6. Vilimpoc, V., Goss, L. P., and Sarka, B., *Opt. Lett.* 13:93–95 (1988).
7. Vilimpoc, V. and Goss, L. P., *Twenty-Second Symposium (International) on Combustion*, The Combustion Institute, Pittsburgh, 1988, pp. 1907–1914.
8. Goss, L. P., Vilimpoc, V., Sarka, B., and Lynn, W. F., *J. Eng. Gas Tur. Power* 111:46–52 (1989).
9. Chen, T. H., Goss, L. P., Trump, D. D., Sarka, B., Vilimpoc, V., Post, M. E., and Roquemore, W. M., in *FED—Flow Visualization* (B. Khalighi, M. J. Braun, and C. J. Freitas, Eds.), The American Society of Mechanical Engineers, New York, 1989, Vol. 85, pp. 121–127.
10. Bédat, B., Giovannini, A., and Pauzin, S., *Expts. Fluids* 17:397–404 (1994).
11. Incropera, F. P. and DeWitt, D. P., *Introduction to Heat Transfer*, 2nd ed., Wiley, New York, 1990.
12. Richardson, T. F. and Santoro, R. J., Personal Communication, 1993.

COMMENTS

Fumiaki Takahashi, University of Dayton, USA. A common problem encountered when inserting a physical probe into sooting flames is the accumulation of soot (and precursors) on the probe. In thin-filament pyrometry, such an event may alter the emissivity of the filament, increase the filament diameter, and eventually disturb the flow field. How did you overcome this problem?

Author's Reply. During this study the deposition of soot on the SiC filament was observed for a limited number of experiments, leading to variations in the emission intensity and thus the measured filament temperatures. Soot deposition was most obvious for steady laminar flames, and, for this reason, calibrations were recorded near the base of the flame where soot had not yet formed. In the time-varying methane flame, evidence for soot deposition was limited to a very few phases and downstream positions, despite the fact that soot volume fractions are known to reach values of 1.8×10^{-6}. This observation likely results from the movement of the high-temperature reaction zone along the filament during each flickering cycle. Apparently, in most cases, any soot which is deposited on the filament at a particular location is immediately burned away during the same or subsequent cycle and soot does not have an opportunity to accumulate significantly. Support for this conclusion comes from the observation that large deposits of soot on the filament could be removed by placing the filament in downstream regions of the time-varying flame and allowing the soot to burn off.

•

Viswanath R. Katta, Innovative Scientific Solutions Inc., USA. Accuracy of temperature measurements using thin-filament-pyrometry technique strongly depends on the velocity used in the correction process. In flickering buoyant flames, velocity fluctuations are quite significant. Without the knowledge of the history of the velocity fluctuations, reduction of temperature from the filament signal leads to large errors. Time-accurate measurements for velocity in these flames are equally difficult. How is the pyrometry technique going to provide accurate temperature information in such flames?

Author's Reply. Dr. Katta correctly points out that converting the semi-quantitative temperature measurements discussed in this manuscript, denoted as "Measured Filament Temperatures," to absolute values will require detailed knowledge of the velocity fields of the time-varying diffusion flames. As noted in the text, it is also necessary to characterize the concentration field. Furthermore, a calibration flame system in which the temperature field is well known and for which velocities and composition have been mapped out is required as well. We have not yet attempted to make these corrections. The velocities could be obtained by measurements using LDV or PIV or from modeling calculations such as those recently reported by Kaplan et al. [1] for the current flame system. Similarly, the concentration field could be measured experimentally or estimated using modeling approaches, e.g., the laminar flamelet concept along with detailed kinetic modeling. Perhaps the most difficult task is developing an appropriate calibration flame since temperature characterization with the required accuracy of a few degrees is extremely difficult. An estimate of the ultimate accuracy which can be achieved requires a careful error analysis based on all possible sources of uncertainty.

REFERENCE

1. Kaplan, C. R., Shaddix, C. R., and Smyth, K. C., *Combust. Flame* 106:393–405 (1996).